NASA TN D-994

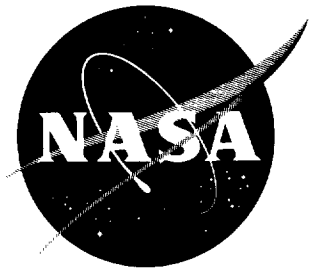

TECHNICAL NOTE

D-994

AERODYNAMIC CHARACTERISTICS OF TOWED CONES USED AS DECELERATORS AT MACH NUMBERS FROM 1.57 TO 4.65

By Nickolai Charczenko and John T. McShera

Langley Research Center
Langley Air Force Base, Va.

NATIONAL AERONAUTICS AND SPACE ADMINISTRATION

WASHINGTON December 1961

NATIONAL AERONAUTICS AND SPACE ADMINISTRATION

TECHNICAL NOTE D-994

AERODYNAMIC CHARACTERISTICS OF TOWED CONES USED AS DECELERATORS AT MACH NUMBERS FROM 1.57 TO 4.65

By Nickolai Charczenko and John T. McShera

SUMMARY

Towed and sting-supported cones were tested in the wake of various payloads at supersonic speeds to determine their drag and stability characteristics. The investigation extended over a Mach number range from 1.57 to 4.65 and included such variables as Reynolds number, cone angle, ratio of cone base diameter to payload base diameter, and trailing distance.

The results of this investigation showed that the cones towed in the wake of a symmetrical payload at supersonic speeds, in general, have good drag and stability characteristics if towed in the supersonic flow region.

A cone with an included angle between 80° and 90° will give maximum drag while still maintaining stability in the Mach number region of this investigation. In order to minimize wake effects, the ratio of cone base diameter to payload base diameter should be at least one and preferably around three. A trailing distance of three times the payload base diameter, in most cases, is of sufficient length to avoid low drag and instability of the decelerator.

INTRODUCTION

The investigation discussed herein is part of an overall program to study possible decelerator configurations capable of providing satisfactory deceleration performance at supersonic speeds. Such decelerators would be employed for the recovery of spacecraft, launch vehicles, and other high-speed vehicles. Parachutes, balloons, retrorockets, conical rings, and cones are some of the drag devices that are being considered as decelerators. (See refs. 1 to 3.) All of these drag devices have certain advantages and disadvantages, and the final selection for a particular application will be based upon such factors as weight, drag coefficient, stability, and simplicity of design. Because of the geometric simplicity of cones and their wide application,

aerodynamic characteristics of cones have been studied extensively and are comparatively well understood. The use of cones as towed decelerators, however, introduces factors that require study inasmuch as these cones are in the wake of a payload and their usefulness will be limited to the flow regions and cone angles resulting in satisfactory decelerator characteristics. Cones were tested over a Mach number range from 1.57 to 4.65 to determine the effect of Reynolds number, cone angle, relative size of the cone with respect to the payload, and trailing distance on the drag coefficient of a cone in the wake of a payload.

SYMBOLS

A	cone base area, sq ft
C_D	drag coefficient, $\frac{\text{Drag}}{q_\infty A}$
$C_{D,p}$	pressure drag coefficient, $\frac{p_l - p_\infty}{q_\infty} \cdot \frac{A}{A}$
d_p	payload base diameter, in.
d_c	cone base diameter, in.
l	tow-cable length (fig. 3), in.
l/d_p	trailing distance in terms of payload base diameters
d_c/d_p	ratio of cone base diameter to payload base diameter
M_∞	free-stream Mach number
p_l	local pressure, lb/sq ft
p_∞	free-stream static pressure, lb/sq ft
q_∞	free-stream dynamic pressure, lb/sq ft
θ	cone angle (see fig. 3), deg

APPARATUS AND MODELS

Wind Tunnel

The tests were conducted in the Langley Unitary Plan wind tunnel, which is a variable-pressure return-flow tunnel. The tunnel has two test sections which are 4 feet square and approximately 7 feet in length. The nozzles leading to the test sections are asymmetric sliding-block-type nozzles, and the Mach number may be varied continuously through a range from 1.5 to 2.8 in one test section and from 2.3 to 4.65 in the other. Further details of the wind tunnel may be found in reference 4.

Models

A sketch and photographs of the test section and payload support system are shown in figure 1. The support system consisted of two thin struts spanning the tunnel in the horizontal plane. The payload was held in the center of the tunnel by these struts. The three types of payloads used in this investigation are shown in figure 2. Payload A had a flared body with the flare starting at the termination of the nose cone and extending to the base; payload B had a cylindrical body, and payload C had a cylindrical body with flared afterbody. The payloads were tested under the conditions indicated in table I. The two different size 60° cones tested with payload A were sting mounted on a movable strut with the balance inside the cone. During most of the runs a rod 1/2 inch in diameter, which extended from the vertex of the cone to the base of the payload, was attached to the cone to simulate a tow cable. The drag coefficients obtained for sting-mounted cones tested behind payload A were not corrected for sting interference. The payloads B and C had the balance located inside them. Cones tested with these payloads (see table I) were attached with a 1/16-inch tow cable to a drum which was mounted on the balance inside the payload (see figs. 1 and 3). The balance with the motor-driven drum comprised a convenient system for testing towed decelerators since the distance between payload and cone could be varied during the test without tunnel shutdown. The existence of rough flow as well as back flow in the test section during the starting and shutdown of the tunnel necessitated the adoption of some means to stabilize the cone during these periods. A string tied from the back of the cone to the knuckle on the movable strut prevented the cone from striking the test-section wall or wrapping around the supporting strut. This string was slack during the test so that it had little interference on the cone.

TESTS AND ACCURACIES

Most of the drag coefficients presented herein for both sting-mounted and towed cones are for a Reynolds number per foot of approximately 3×10^6. Reynolds number effect was determined for one configuration by a change in tunnel stagnation pressure. Table I presents the cone-payload combinations and the Mach numbers at which they were tested.

The accuracy of the individual quantities and coefficients is estimated to be within the following limits:

C_D	±0.02
l, in.	±0.5
M_∞ (1.57 to 2.87; test section 1)	±0.02
M_∞ (2.30 to 4.65; test section 2)	±0.05

RESULTS AND DISCUSSION

Pressure Drag on Cones

The drag of a cone consists primarily of pressure drag with a small contribution of skin-friction drag. The pressure drag of a cone is composed of forebody pressure drag, which can be readily determined from theory, and base pressure drag, which is difficult to evaluate by theoretical means even for the most simple case. The forebody pressure drag as determined by the shock-wave theory for several cone angles and some experimental base pressure drag data for 60° cones are presented in figure 4 along with the base drag associated with zero base pressure. The boundary shown for the forebody indicates detachment of the shock from a cone, which in the case of towed cones is accompanied by loss of drag and stability. The base drag could amount to a considerable portion of the total pressure drag of a cone at lower Mach numbers; however, with increasing Mach number the importance of base pressure drag rapidly diminishes.

Although large increments in drag can be gained by increasing the cone angle, there is an accompanying decrease in stability that would be expected from the theory of reference 5. In the present investigation it was found that the stability of the cone approaches its critical value in the neighborhood of $\theta = 90°$. This finding does not imply that 90° is the maximum cone angle that can be used in cone-decelerators, inasmuch as there is no well-defined boundary that determines stable and unstable cones. Even though the stability of a 90° cone improved slightly at higher Mach numbers and longer tow-cable lengths, the 90° cone was not as stable as cones having lesser cone angles.

Measured Drag on Towed and Sting-Mounted Cones

Reynolds number effect on the drag coefficient of a 60° cone.- The data presented in this paper are confined to a range of Reynolds numbers per foot of approximately 3×10^6 to 6×10^6. The 60° cone tested in the wake of payload A at Mach numbers of 1.57 and 2.00 showed no Reynolds number effect on the drag coefficient, as can be seen in figure 5. The small difference in drag coefficients of a 60° cone at a Mach number of 2.00 is within the experimental accuracy. Similar results were obtained in reference 6, where a 30° cone was tested in the free stream at a Mach number of 2.41. The transition region shown in figure 5 characterizes the type of flow field surrounding the cone; this region will be discussed in subsequent paragraphs.

L
1
5
0
5

Effect of relative size of the decelerator with respect to the payload.- The drag coefficient for two 60° cones of different base diameters is shown in figure 6. Both cones had smaller base diameters than the payload; the larger of the cone diameters was 86 percent and the smaller 66 percent of the payload A base diameter. Even though the difference in size between the two cones was not very large, there were some significant trends that could be observed in figure 6. The drag coefficient was higher for the larger cone throughout the l/d_p range at all Mach numbers, and a small increase in the C_D increment was noticeable with increase in Mach number. Since the two cones were geometrically similar and Reynolds number effects were negligible, they should have the same drag coefficient in an undisturbed free stream. However, the cones were located in the wake of the payload, and as a result they experienced a somewhat different flow field because of their relative size with respect to the payload. Thus the difference in the drag coefficient for these two cones can be attributed primarily to the wake effects of the preceding body. Similar results are observed in figure 7 where a 60° cone was towed behind payloads B and C with ratios of cone base diameter to payload base diameter of 2.05 and 0.88, respectively. Note that payloads B and C had different shapes; this difference in shape would probably have some influence on the drag coefficient. Based on the present tests and limited amount of other data available, the ratio of decelerator base diameter to payload base diameter should be at least equal to or greater than one and preferably around three (ref. 7).

Effect of tow cable and tow-cable length on the drag of decelerators.- The effect of a tow cable on the drag of a cone was determined with a rod simulating the tow cable and attached to a sting-supported 60° cone. The cone was tested in the wake of payload A at three free-stream Mach numbers and at trailing-distance ratios l/d_p from 2 to 6. Results, as shown in figure 8, indicate that the rod caused a small reduction in drag at all three Mach numbers for values of l/d_p greater than 3; for

l/d_p values less than 3, no difference in drag was observed. The slight reduction in drag due to the rod is not significant in itself; but the presence of the rod becomes important at higher cone angles or as the cones approach the critical Mach number at which separation of the shock from the vertex of a cone occurs (see fig. 4). The presence of the rod causes a detachment of shock to occur at higher Mach numbers than for the cone alone in the free stream, and this result produces adverse effects on the drag and stability of a towed cone.

Figures 9 and 10 show the flow field for various cones behind payload C at several Mach numbers. At supersonic speeds the wake from a payload can be divided into three regions. As the downstream distance from the payload increases, these regions may be defined as subsonic, transition, and supersonic regions, each having a distinct characteristic.

In the subsonic region a towed cone may be completely immersed in the wake of the payload and its behavior characterized by low drag and a lack of stability. For example, only the 60° cone was sufficiently stable to be tested in this region; all others, 70°, 80°, and 90° cones, were unstable. A schlieren picture of a 60° cone operating in this flow region is shown in figure 9 $\left(l/d_p = 2.0\right)$.

The transition region is where the flow field in front of a cone changes from subsonic to supersonic or vice versa. Location of this region behind the payload will depend upon the ratio of payload base diameter to cone base diameter, payload shape, and the free-stream Mach number. A good example of this region is shown in reference 8, where 60° and 90° sting-supported cones were tested in the wake of a payload at free-stream Mach numbers from 1.5 to 6. In the present investigation, drag data for towed cones could not be obtained in the transition region because the cones were extremely unstable in this region. For a given payload and decelerator, the transition-region location is primarily a function of Mach number which, of course, changes throughout the payload trajectory. In order to determine the minimum tow-cable length that is required to avoid the transition region, it would be necessary to establish only the most rearward point of the transition region in the trajectory. For the configurations investigated, in no case did the transition point occur for values of l/d_p greater than 3; therefore, a tow-cable length equal to three times the payload base diameter should be of sufficient length to avoid both the subsonic and transition regions.

The supersonic region is characterized by high drag (approximately twice that in the subsonic region) and good stability for cones having included angles up to about 90°. In this region the variation in drag with increasing trailing distance is small, as can be seen in most of the figures.

In order to minimize adverse wake effects on the drag of a cone, there are two design variables that can be selected: either the tow-cable length can be increased to place the cone where the wake effects are small, or the size of the decelerator with respect to the payload can be increased. In either case, increasing the length of a tow cable beyond the transition region or increasing the size of a cone will add weight which will have to be justified by the increase in drag thus obtained.

Effect of cone angle.- The expected drag-coefficient increase with increase in cone angle can be seen in figure 11 for all cones except the 90° cone at a Mach number of 2.30 and the 90° cone at Mach numbers of 2.96 and 4.65 for short tow-cable lengths. The low drag values for the 90° cone are believed to have been caused by the detachment of a shock from the cone. Schlieren photographs indicate that the detachment of shock from the 90° cone in the payload wake occurred at higher Mach numbers than is shown in figure 4. The detachment of a shock from the 90° cone at higher Mach numbers was probably caused by both the presence of the tow cable and the flow field surrounding the cone, since this flow field was different from that of the free stream on which figure 4 was based. At a Mach number of 4.65 and $\frac{l}{d_p} = 2.8$ there was also a detachment of shock from the 90° cone (fig. 10(c)); however, in this instance the impingement of the trailing shocks from the payload on the cone was probably the major cause. Visual observations in the course of this investigation showed that the stability of the cones decreased with increasing cone angle. The 90° cone could not be considered entirely stable inasmuch as its stability varied between violent oscillations and relatively calm periods. Thus, the 80° cone would probably be more suitable as a decelerator, although some drag may be compromised for stability.

The low drag-coefficient values (indicated in fig. 11) at a Mach number of 2.30 for 60° and 80° cones and l/d_p of 6.0 and 6.8, respectively, were caused by the sting support influencing the base pressure of the cones. This effect can be seen in the schlieren photograph shown in figure 9 for the 60° cone. No suitable explanation was found for the decrease in drag coefficient with increase in l/d_p at free-stream Mach numbers of 3.83 and 4.65 (fig. 11). Similar effects were observed in reference 8 for a 90° cone between Mach numbers of 3 and 5.

CONCLUSIONS

The investigation of 60°, 70°, 80°, and 90° cones used as decelerators at supersonic speeds in the wake of several payloads has led to the following conclusions:

1. A cone with an included angle between 80° and 90° would be most suitable for use as a decelerator in the Mach number regions of this investigation. From visual observations in the course of this investigation it was established that the stability of the cones decreased with increasing cone angle. The 90° cone was intermittently unstable at the test Mach numbers.

2. For the configurations investigated at Mach numbers up to 4.65, a trailing distance of three payload base diameters would be sufficient to avoid low drag and instability regions of the decelerator.

3. The ratio of cone base diameter to payload base diameter should be at least equal to or greater than one in order to minimize adverse wake effects.

4. The presence of the tow cable had little influence on the drag coefficient of a cone except at large cone angles and at critical Mach numbers where shock detachment from the cone took place. In these instances the tow cable caused detachment of the shock at higher Mach numbers than would be expected from the shock-wave theory, and this result produced adverse effects on the drag and stability of the cone.

Langley Research Center,
National Aeronautics and Space Administration,
Langley Air Force Base, Va., September 27, 1961.

REFERENCES

1. Maynard, Julian D.: Aerodynamic Characteristics of Parachutes at Mach Numbers From 1.6 to 3. NASA TN D-752, 1961.

2. McShera, John T., and Keyes, J. Wayne: Wind-Tunnel Investigation of a Balloon as a Towed Decelerator at Mach Numbers From 1.47 to 2.50. NASA TN D-919, 1961.

3. Charczenko, Nickolai, and Hennessey, Katherine W.: Investigation of a Retrorocket Exhausting From the Nose of a Blunt Body Into a Supersonic Free Stream. NASA TN D-751, 1961.

4. Anon.: Manual for Users of the Unitary Plan Wind Tunnel Facilities of the National Advisory Committee for Aeronautics. NACA, 1956.

5. Fisher, Lewis R.: Equations and Charts for Determining the Hypersonic Stability Derivatives of Combinations of Cone Frustums Computed by Newtonian Impact Theory. NASA TN D-149, 1959.

6. Grigsby, Carl E., and Ogburn, Edmund L.: Investigation of Reynolds Number Effects for a Series of Cone-Cylinder Bodies at Mach Numbers of 1.62, 1.93, and 2.41. NACA RM L53H21, 1953.

7. Maynard, Julian D.: Aerodynamics of Decelerators at Supersonic Speeds. Proc. of Recovery of Space Vehicles Symposium (Los Angeles, Calif.), Inst. Aero. Sci., Sept. 1960, pp. 48-54.

8. Coats, Jack D.: Static and Dynamic Testing of Conical Trailing Decelerators for the Pershing Re-Entry Vehicle. AEDC-TN-60-188 (Contract No. AF 40(600)-800 S/A 11(60-110)), Arnold Eng. Dev. Center, Oct. 1960.

9. Kurzweg, H. H.: New Experimental Investigations on Base Pressure in the NOL Supersonic Wind Tunnels at Mach Numbers 1.2 to 4.24. Naval Ordnance Lab. Memo. 10113, Jan. 23, 1950.

TABLE I.- TEST CONDITIONS

Payload	Payload base diameter, d_p, in.	Cone base diameter, d_c, in.	Cone angle, θ, deg
Test section 1: M_∞ of 1.57, 2.00, and 2.87			
A	4.9	4.210	60
A	4.9	3.240	60
Test section 2: M_∞ of 2.30, 2.96, 3.83, and 4.65			
B	2.4	4.875	60
C	5.5	4.875	60
C	5.5	4.875	70
C	5.5	4.875	80
C	5.5	4.875	90

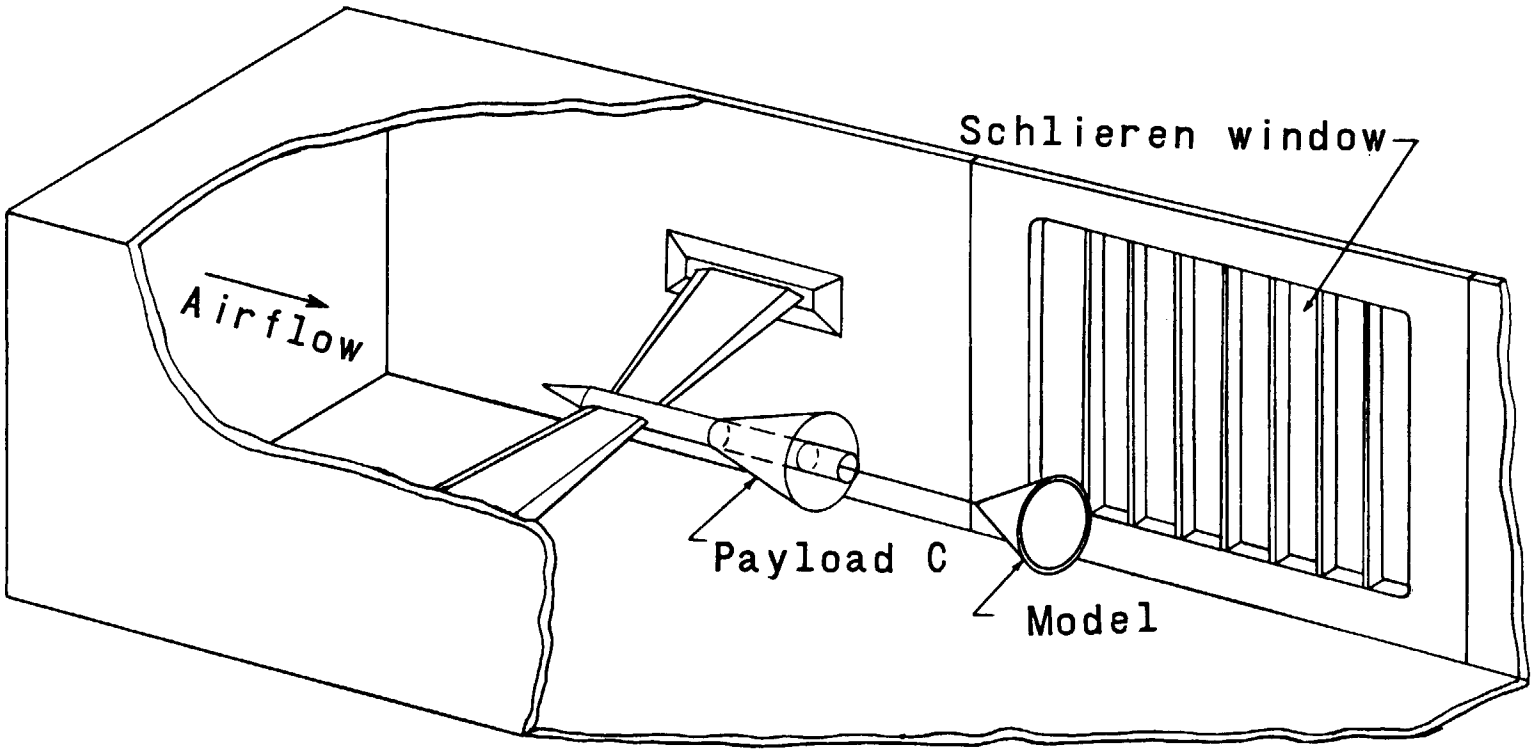

(a) Sketch of payload C mounted on a strut.

Figure 1.- Sketch and photographs showing payloads and the support system.

L-60-4419

L-60-4421

(b) Photographs of payload B mounted on a strut.

Figure 1.- Concluded.

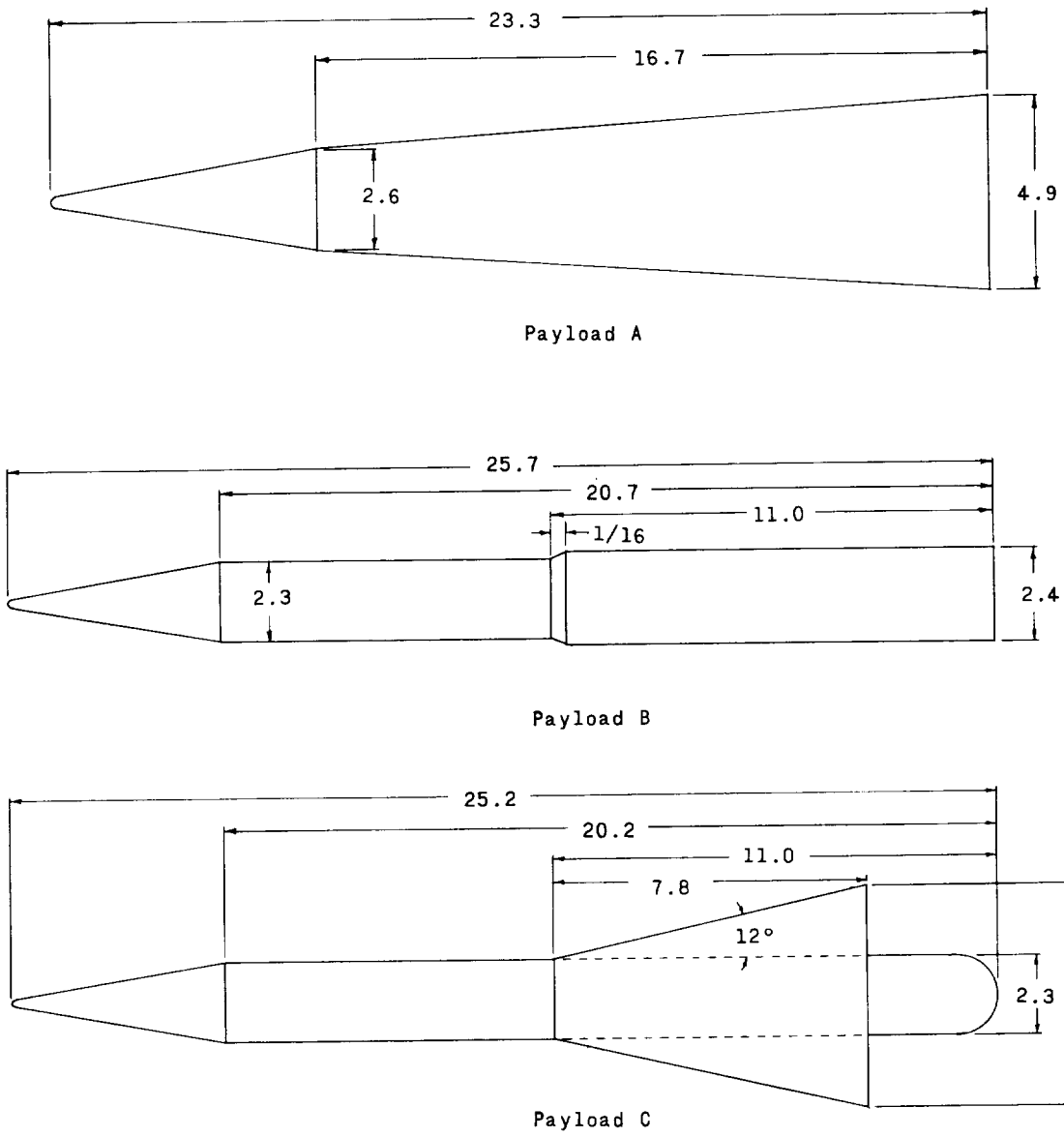

Figure 2.- Drawing of three types of payloads used in this investigation. All linear dimensions are in inches.

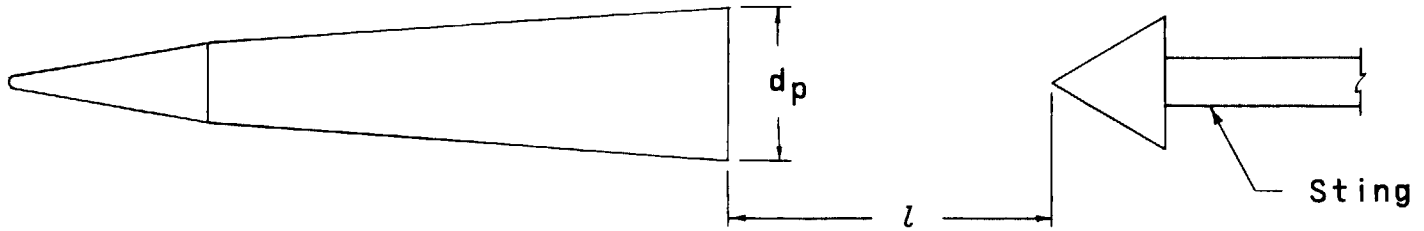

Sting-supported cone

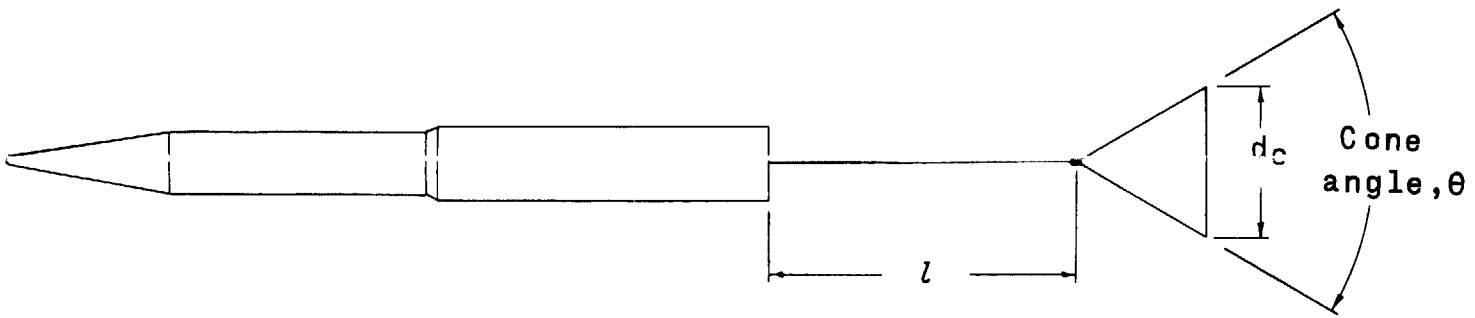

Towed cone

Figure 3.- Sketch of two types of cone attachments used.

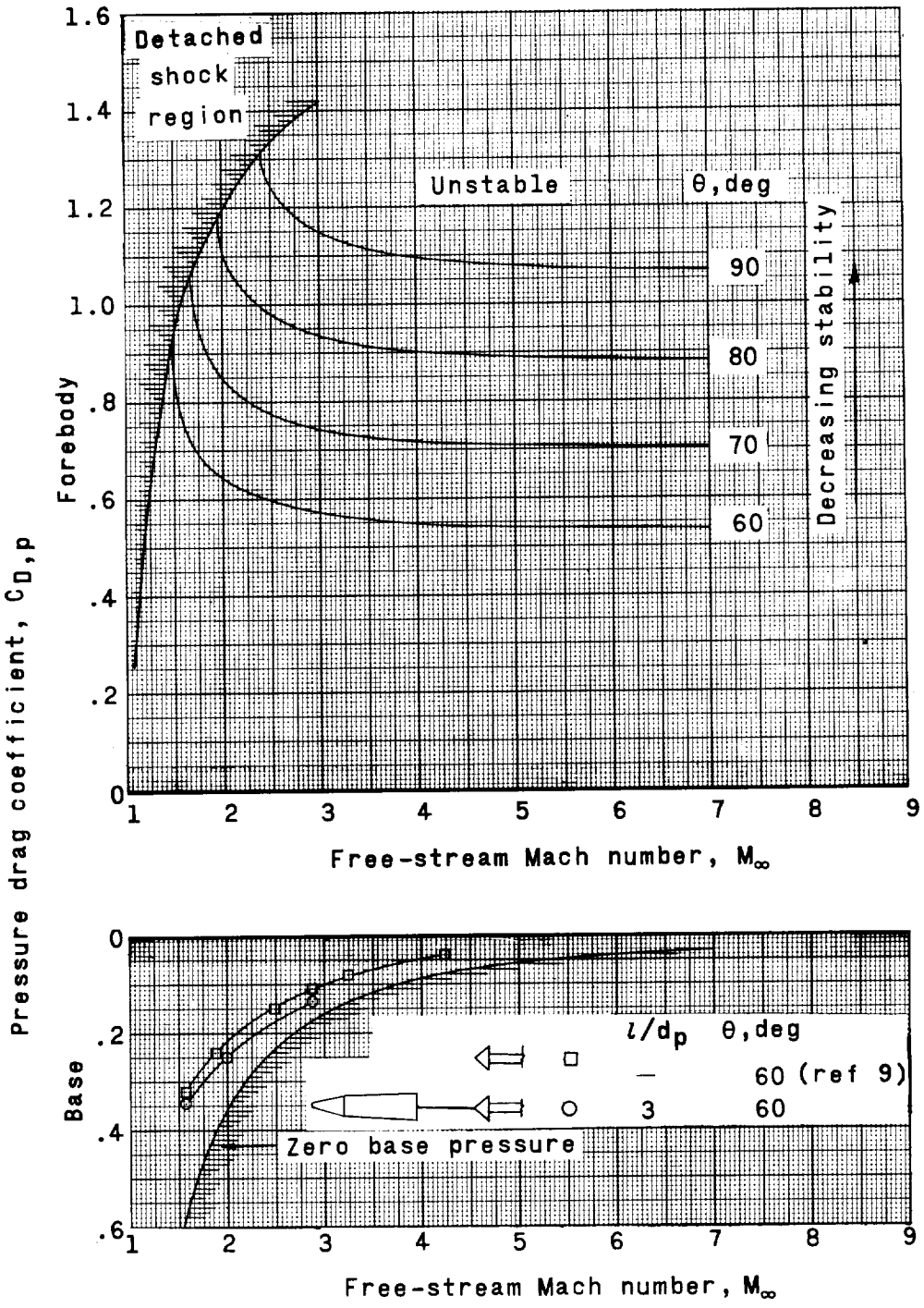

Figure 4.- Variation of pressure drag coefficient with Mach number for different cone angles.

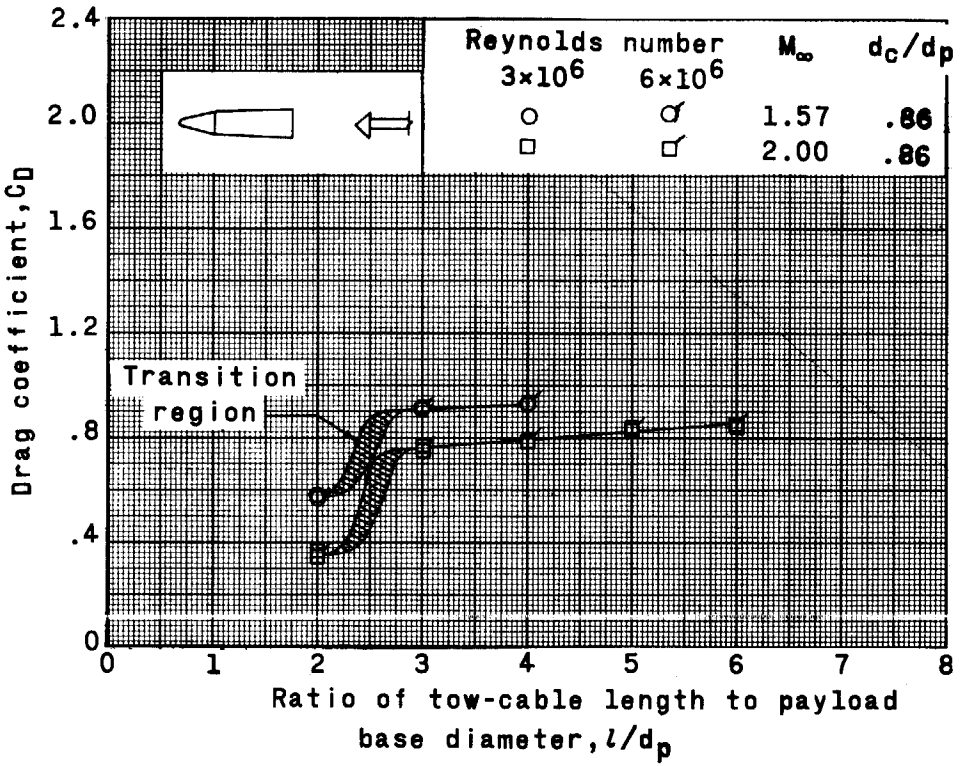

Figure 5.- Effect of Reynolds number on the drag coefficient of a 60° cone tested in wake of payload A at two free-stream Mach numbers.

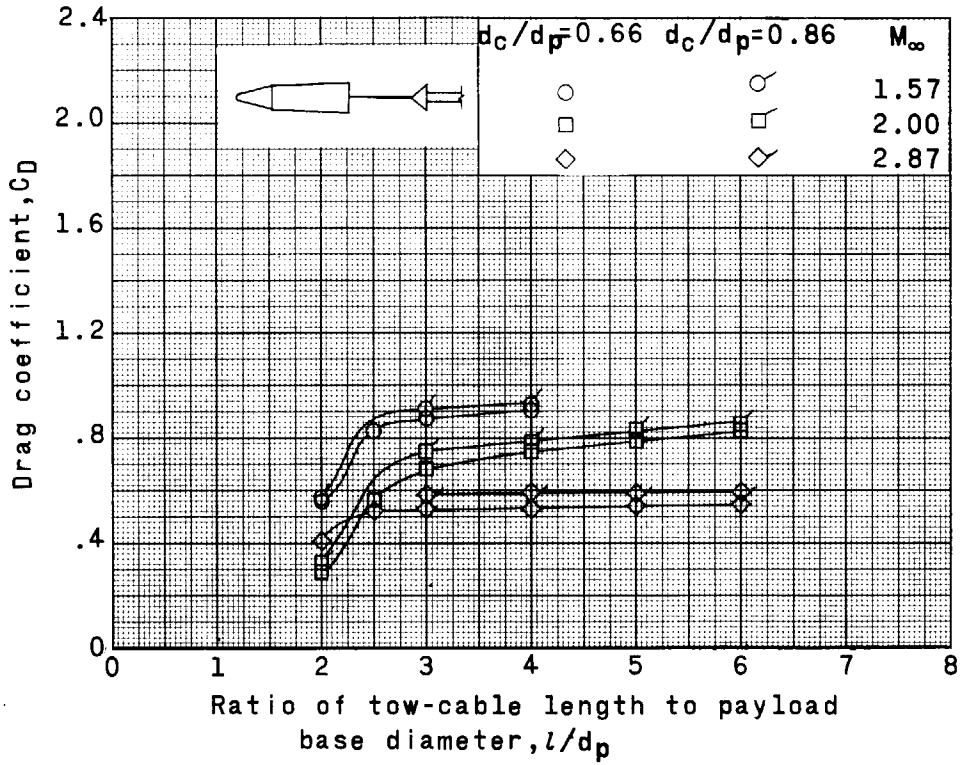

Figure 6.- Effect on drag coefficient of the size of a 60° cone tested in the wake of payload A at three Mach numbers.

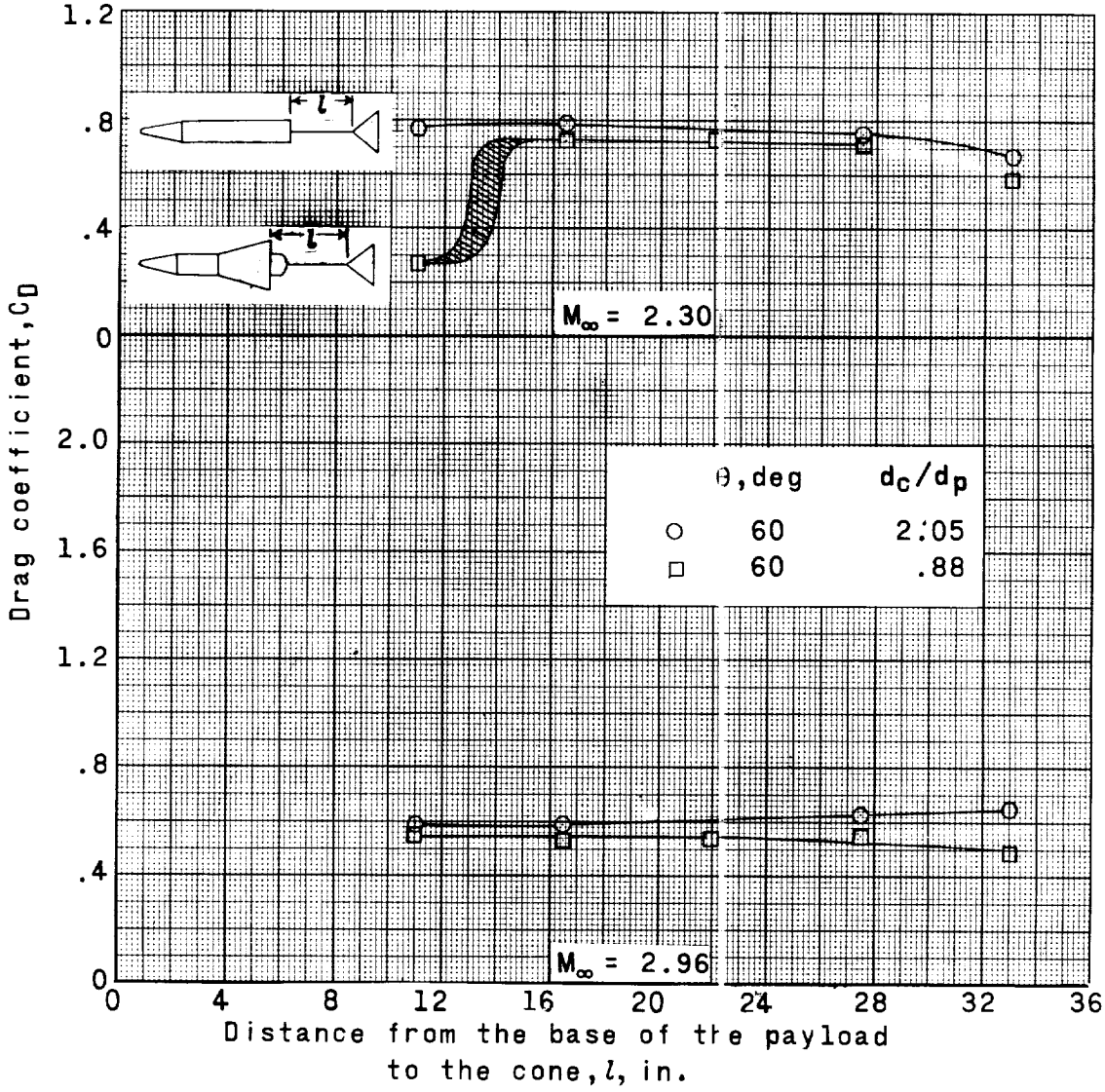

Figure 7.- Effect of payload on the drag coefficient of a 60° cone. $\frac{d_c}{d_p}$ = 2.05 for payload B and 0.88 for payload C.

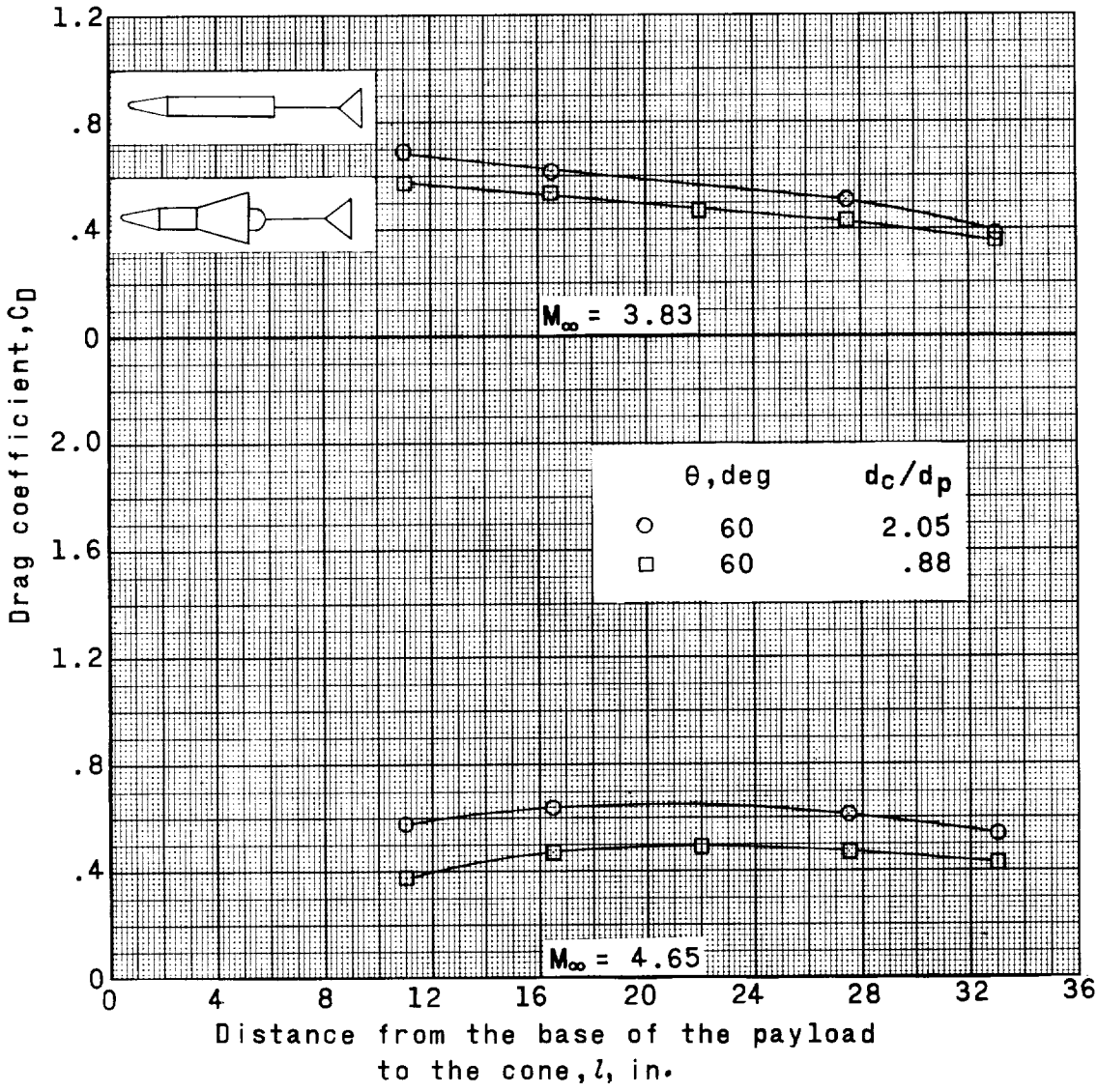

Figure 7.- Concluded.

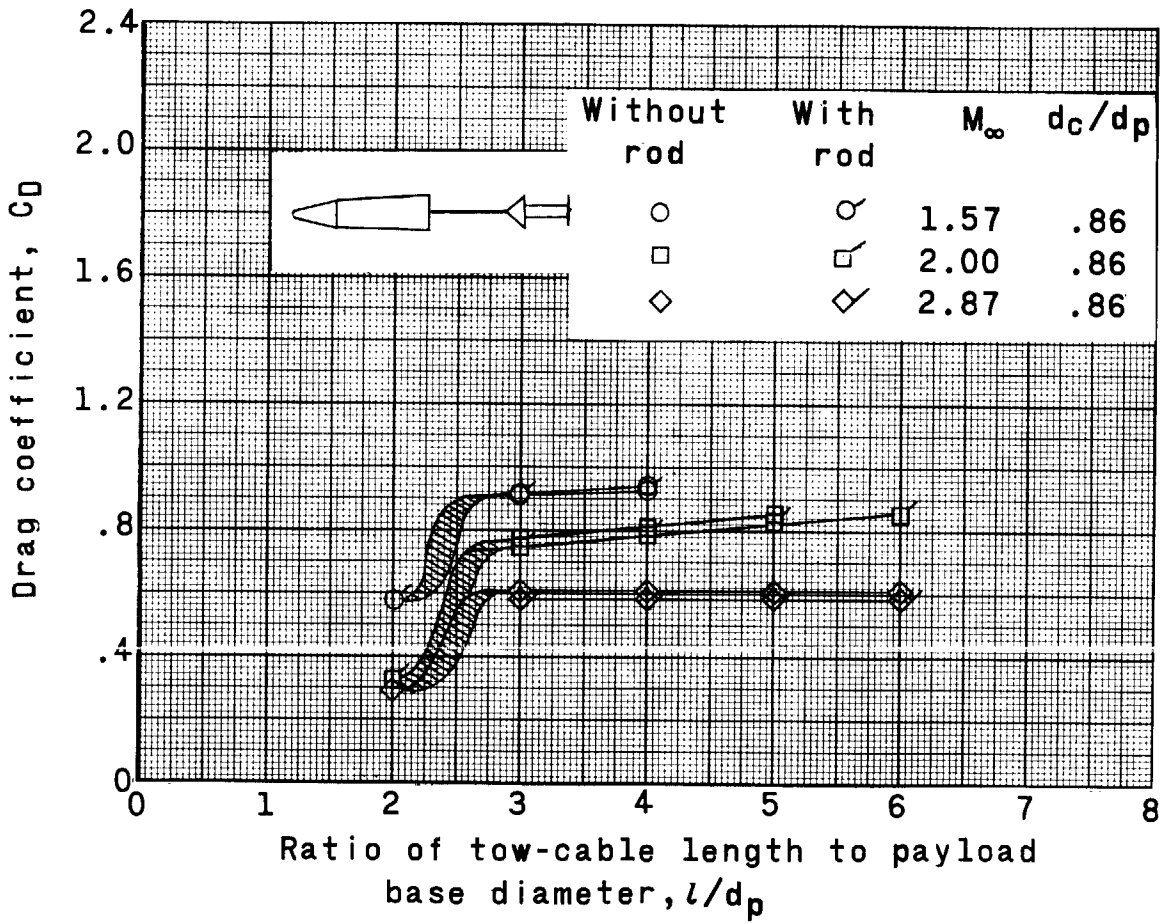

Figure 8.- Effect of the simulated tow cable on the drag coefficient of a 60° cone tested behind payload A.

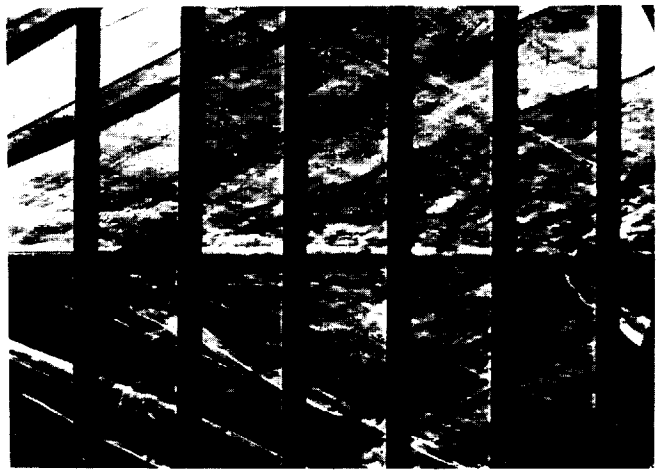

l/d_p = 2.0

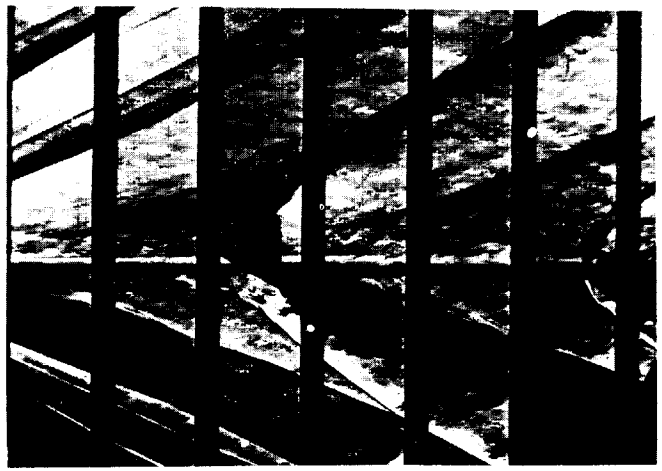

l/d_p = 3.0

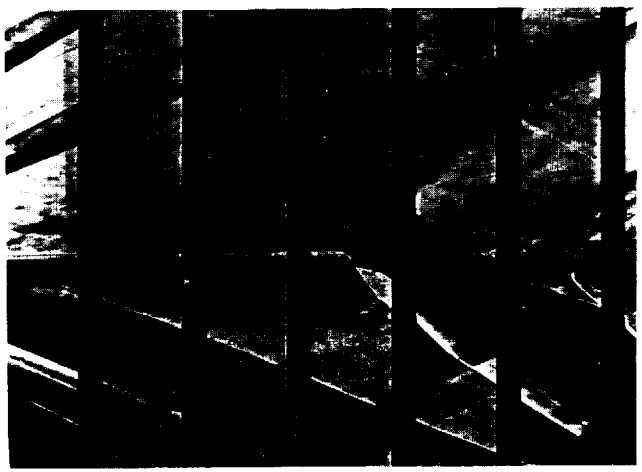

l/d_p = 5.0

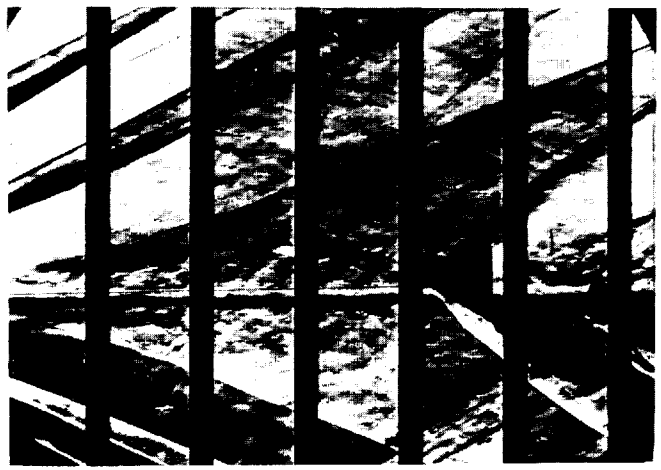

l/d_p = 6.0

Figure 9.- Flow field about a 60° cone behind payload C at M_∞ = 2.30. L-61-5111

l/d_p = 2.0; θ = 60°

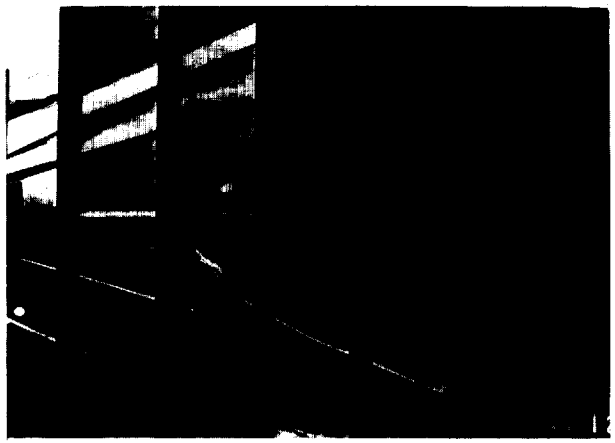

l/d_p = 2.0; θ = 70°

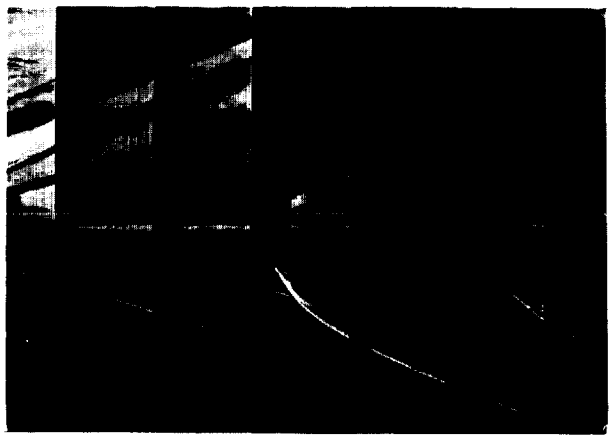

l/d_p = 2.8; θ = 80°

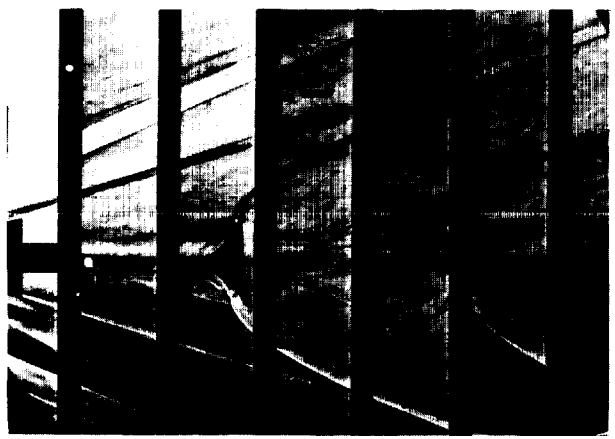

l/d_p = 2.3; θ = 90°

(a) M_∞ = 2.96. L-61-5112

Figure 10.- Flow field about various cones behind payload C.

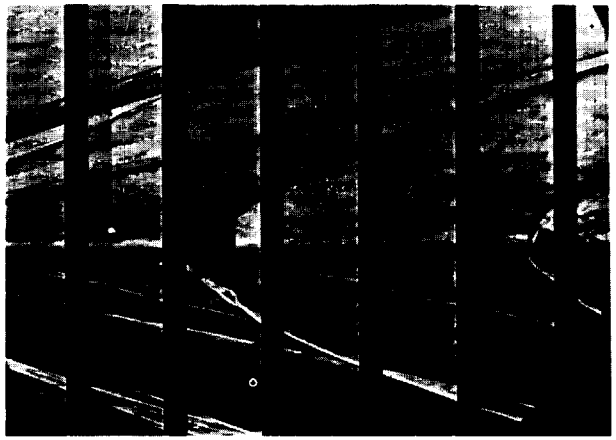

l/d_p = 3.0; θ = 60°

l/d_p = 2.8; θ = 70°

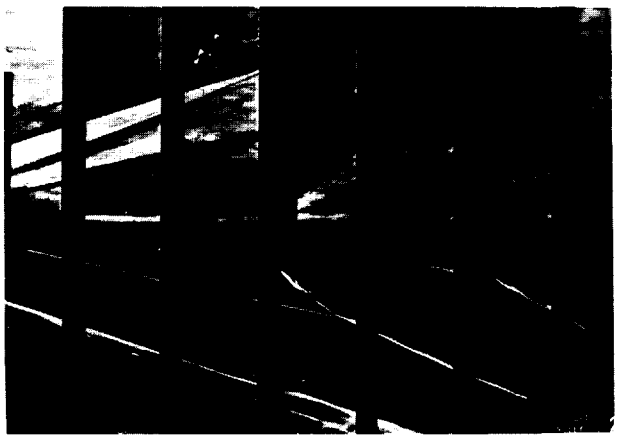

l/d_p = 2.8; θ = 80°

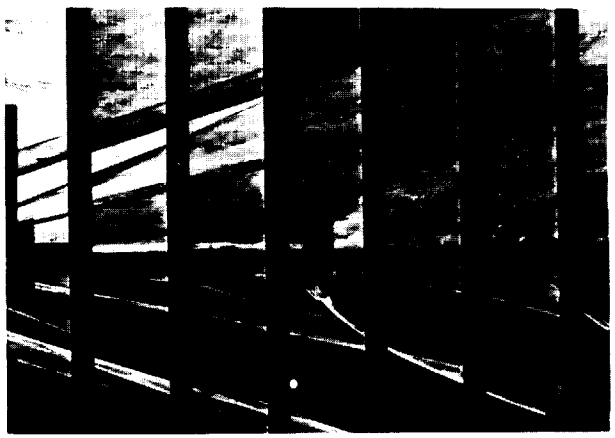

l/d_p = 3.0; θ = 90°

(b) M_∞ = 3.83. L-61-5113

Figure 10.- Continued.

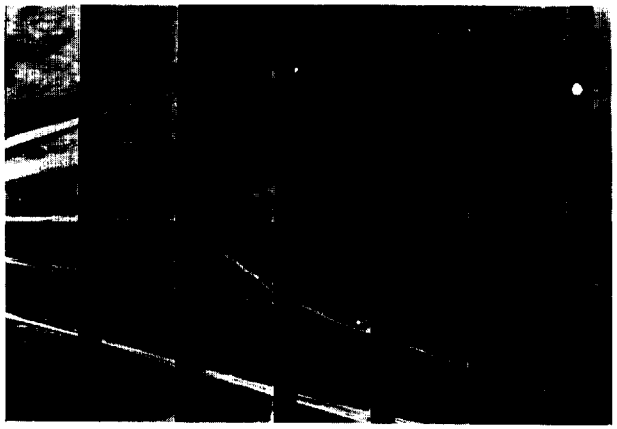

l/d_p = 3.0; θ = 60°

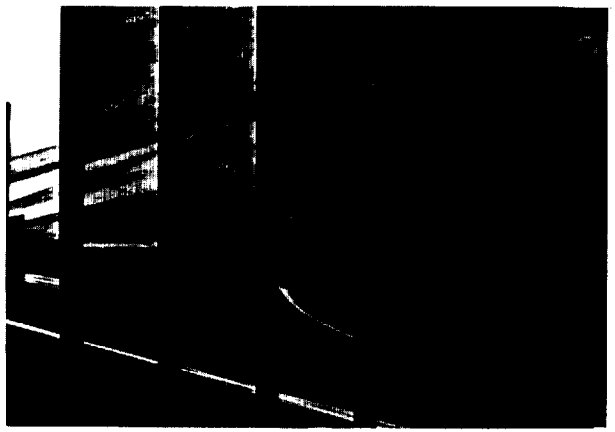

l/d_p = 2.8; θ = 70°

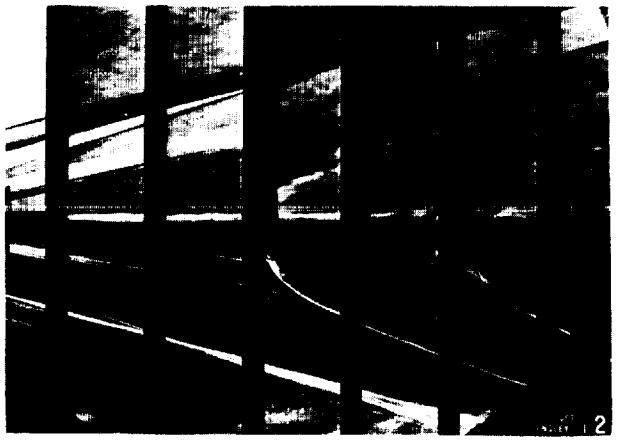

l/d_p = 2.8; θ = 80°

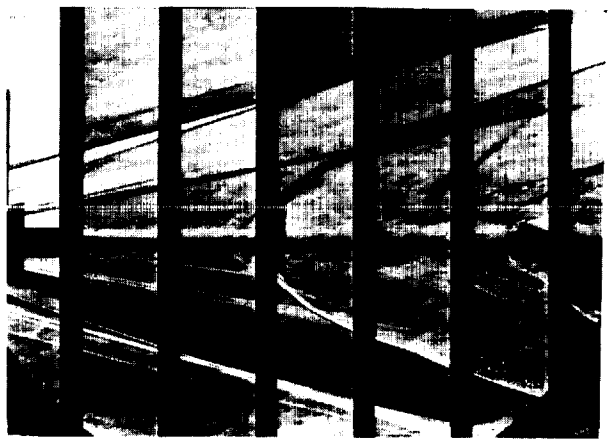

l/d_p = 2.8; θ = 90°

(c) M_∞ = 4.65. L-61-5114

Figure 10.- Concluded.

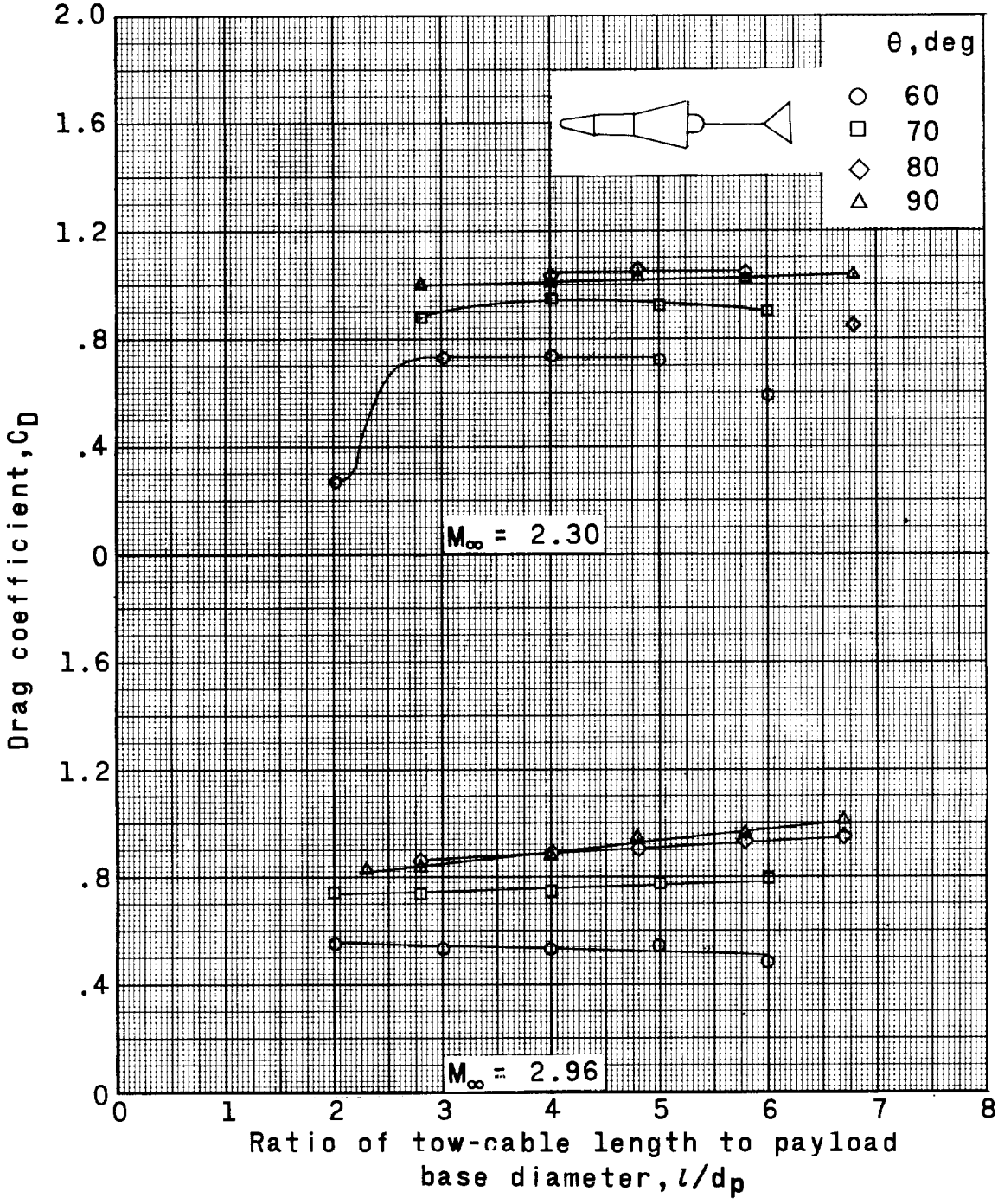

Figure 11.- Variation of drag coefficient with tow-cable length for different cone angles. Cones towed behind payload C.

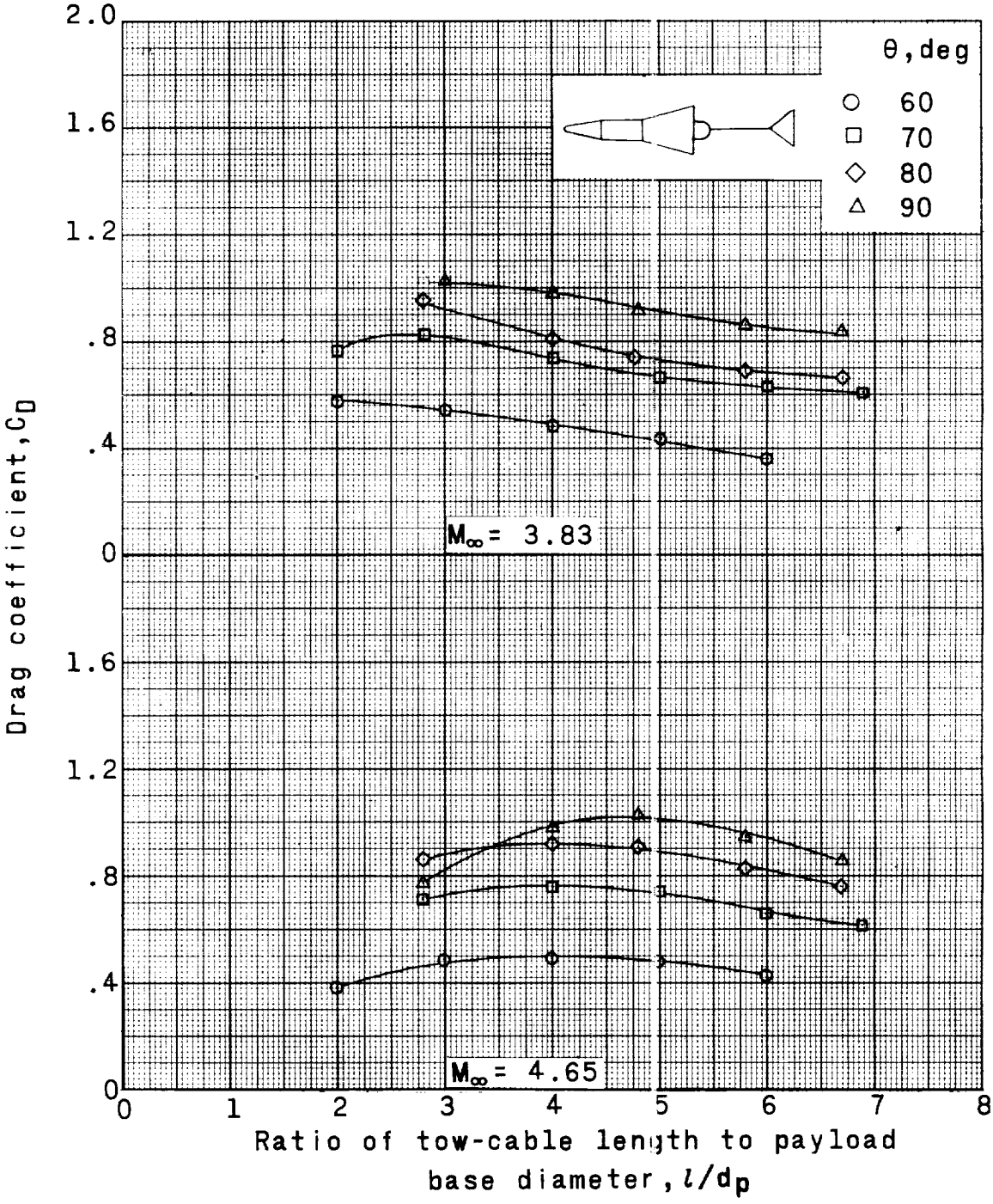

Figure 11.- Concluded.

L-1505